AUT Journal of Mechanical Engineering

AUT J. Mech. Eng., 6(1) (2022) 15-30
DOI: 10.22060/ajme.2021.20283.5995

A Proposed Approach to Simulate Thin Quadrilateral Plates Using Generalized Differential Quadrature Method Based on Kirchhoff–Love Theory

H. Shahverdi*, M. M. Navardi, M. H. Sadr

Department of Aerospace Engineering, Amirkabir University of Technology, Tehran, Iran

ABSTRACT: In this study, an approach to free vibration analysis of thin quadrilateral plates using the generalized differential quadrature method based on the strong version of the governing equation is proposed. Hence, the governing equation of a thin quadrilateral plate is firstly obtained using the Kirchhoff–Love theory of plates (classical theory) to achieve this aim. The well-known differential quadrature method is then utilized to obtain the discretized form of the equations of motion. However, simulation of any arbitrary geometry using conventional Generalized Differential Quadrature Method based on classical theory is impossible. This drawback can be removed by defining the additional degrees of freedom in boundaries. Moreover, the combination of the Refined Differential Quadrature Method with geometry mapping is developed to simulate thin quadrilateral plates. Also, the multi-block or elemental strategy is implemented for problems with more geometric complexities. For this aim, geometry can be divided into several subdomains. Continuity conditions make the connection between adjacent elements at each interface. By establishing the whole discretized governing equations, the free vibration analysis of a thin plate will be provided via the achieved eigenvalue problem. The obtained results are compared and validated with available results in the literature that show high accuracy and a fast rate of convergence.

Review History:

Received: Jul. 21, 2021
Revised: Oct, 19, 2021
Accepted: Oct, 20, 2021
Available Online: Oct, 26, 2021

Keywords:

Continuity condition
Differential quadrature method
Element
Quadrilateral plate
Thin plate

1- Introduction

The free vibration analysis of structures, including any arbitrary shape such as any geometric discontinuities/ complexities and complicated boundary conditions, is one of the attractive problems in the field of mechanical engineering. However, powerful numerical tools such as the Finite Element Method (FEM) can be used to solve the aforementioned problems. In recent decades the development of numerical tools with low computational complexity and high accuracies such as mesh-free method, boundary element method, and Differential Quadrature Method (DQM) has been considered for such problems. The differential quadrature was first introduced by Bellman and Casti [1]. This method has many positive features such as less complexity, faster convergence, and higher accuracy than other numerical methods for solving the various mechanical problem, especially in simple domains expressed by partial differential equations [2-3]. Based on the essence of DQM, the partial derivative of a field variable at a specified point is estimated by a linear summation of the weighted values of the field variable at all discrete points on the domain [2]. The main drawback of the early version of DQM was solved by Shu et al. [4] so that this method was sensitive to the distribution type of sampling points. Therefore, Generalized Differential Quadrature Method (GDQM) was suggested to overcome the expressed drawback based on a polynomial vector space analysis. This method was developed by many researchers converted to a powerful method for solving different mechanical problems so that partial differential equations can include nonlinear terms. Khalafi et al. investigated aeroelasticity analysis of the composite and Functionally Graded Materials (FGM) plates containing linear and nonlinear terms in partial differential equations [5-6]. The presented results indicate the high accuracy and convergence of this method. Wang and Yuan also studied buckling analysis of isotropic skew plates under general in-plane loads using GDQM based on a classical theory with the relations between Cartesian coordinate system and oblique coordinate system [7] so that the governing equation of skew plate was expressed by skewness angle. However, it can be induced that this method is convenient for a simple domain. The structural analysis for complex geometric structures is impossible by using the ordinary GDQ method [3]. Therefore, an elemental approach based on the GDQ method could be appropriate to overcome this problem named Differential Quadrature Elemental Method (DQEM) [8]. The DQEM based on the strong form equation is defined as the manner in which a computational domain is divided into several sub-domains (elements), and the connection between adjacent elements is established in

*Corresponding author's email: h-shahverdi@aut.ac.ir

mathematical form by continuity conditions at boundaries. The DQEM approach was used by many researchers for analyzing various problems containing geometric discontinuity, especially the free vibration of cracked beams [9-10]. The presented results show excellent features such as high accuracy and fast convergence, indicating acceptable compliance between the DQM and elemental approach. However, vast studies were done for beam problems by the DQEM approach. Liu and Liew [11-12] implemented this method to investigate structural analyses of Mindlin's plates containing discontinuity. Afterward, the Generalized Differential Quadrature Finite Element Method (GDQFEM) was introduced to investigate plates' structural analysis with arbitrary shapes by Fantuzzi et al. [13]. They utilized the Mindlin and first-order shear deformation plate theories in their research. The obtained results verify high accuracy and fast convergence. Also, free vibration analysis of cracked plates subjected to a uniaxial in-plane compressive load using GDQM based on Mindlin's theory was conducted by Moradi et al. [14]. Using Mindlin's theory causes three equations of boundary conditions for three governing equations, whereas using Kirchhoff–Love theory causes two equations of boundary conditions for one governing equation. Hence, using the conventional differential quadrature method based on Kirchhoff–Love theory cause regardless of four equations of boundary equations. However, the use of theories related to thick plates is convenient for thin plates; they can increase computational cost because of increasing degrees of freedom. The importance of this problem becomes obvious in the analysis of structure with the high computational cost, such as the optimization process. It is vital that engineers notice to use a suitable theory that fits the model. Therefore, it should be regarded using classical theory for structural analysis of a thin plate. However, a differential quadrature finite element method introduced for free vibration thin beam and plate with arbitrary shape in the weak-form version that led to high accuracy [15], the powerful differential quadrature is known in the strong-form version. The solving of partial differential equations derived by classical theory with the DQEM approach has some restrictions in applying boundary conditions [16]. Many researchers proposed approaches to overcome this difficulty convenient for a single domain [17-18]. Navardi [16] developed the GDQ method for applying different boundary conditions in a thin plate. he suggested extra degrees of freedom at the boundary of a domain to provide three degrees of freedom at corners so that two degrees of freedom were observed at the edge containing displacement and normal slope. The presented results show that this approach had resolved difficulties in applying different boundary conditions, especially when free boundary conditions were applied on two edges perpendicular simultaneously. Shahverdi and Navardi [19] expanded this approach for the elemental approach in order to the simulation of a crack in thin plates. They used six-element for simulation of central crack, and continuity conditions were used for joining elements together. The high accuracy and fast convergence were indicated in this study by the presented results. Thin quadrilateral plates with arbitrary shapes such as skew and trapezial are widely used as a major component in various industries. Hence, structural analysis of such plates is vital to achieving a safe design expressed by a differential equation. Moreover, it is necessary to use a proper method such as the generalized differential quadrature method with the aforementioned positive features than other numerical methods for solving the governing equation [2-3]. Furthermore, the main drawback of the conventional generalized differential quadrature method based on Kirchhoff–Love theory is the imperfection of applying boundary and continuity conditions, especially in the corner points that introduced a refined approach generalized differential quadrature method by Shahverdi and Navardi [19]. However, the only weakness of the proposed method was the simulation and structural analysis of geometries with arbitrary shapes. Therefore, the combination of the geometric mapping and elemental approach in the refined generalized differential quadrature method is developed to solve structures with arbitrary shapes.

The novelty of the present study is to develop an approach based on the Generalized Differential Quadrature Element method (GDQEM) for simulating quadrilateral thin plate structures with mixed boundary conditions based on the classical theory of plates. For this aim, the weighting coefficients are derived in the local coordinate based on GDQM. Then, the weighting coefficients are calculated for all sampling points by geometry mapping in the global coordinate. Finally, the governing differential equations are discretized and presented according to the proposed approach [16, 19] based on GDQEM. The obtained results are evaluated with the available results in the literature.

2- Governing Equations

The equation of motion for a thin structure based on the Kirchhoff–Love theory of plates with regardless of surface shearing forces, body moments, and inertial forces in *x* and *y* direction is presented by [20]:

$$\frac{\partial^2 M_{xx}}{\partial x^2}+2\frac{\partial^2 M_{xy}}{\partial y \partial x}+\frac{\partial^2 M_{yy}}{\partial y^2}+q=I_0\frac{\partial^2 w_0}{\partial t^2} \qquad (1)$$

Also

$$I_0=\int_{-h/2}^{h/2}\rho(z)dz \qquad (2)$$

where M_x, M_y and M_{xy} denote the components of the out-of-plate moment. q and ρ denote the intensity of transverse distributed load and the plate mass density per unit area, respectively. Also, w_0 and I_0 are the transverse displacement and the plate's mass moment of inertia. Based on the classical plate theory, the displacement field of a plate is as follows [20]:

$$u(x,y,z,t)=u_0(x,y,t)-z\frac{\partial w_0(x,y,t)}{\partial x}$$
$$v(x,y,z,t)=v_0(x,y,t)-z\frac{\partial w_0(x,y,t)}{\partial y} \qquad (3)$$
$$w(x,y,z,t)=w_0(x,y,t)$$

Where u, v, and w are the displacement component in the x, y, and z directions, respectively. u_0 and v_0 are the in-plane displacement components, and w_0 is the out-of-plane displacement component of the plate's mid-plane. According to von Karman linear strain-displacement relations, the linear strains are defined as [20]:

$$\{\varepsilon\}=\{\varepsilon^0\}+z\{k\} \qquad (4)$$

where ε^0 and k are the mid-plane membrane and bending strain vectors [20]:

$$\{\varepsilon^0\}=\begin{Bmatrix}\varepsilon_{xx}{}^0\\ \varepsilon_{yy}{}^0\\ \varepsilon_{xy}{}^0\end{Bmatrix}=\begin{Bmatrix}\frac{\partial u_0}{\partial x}\\ \frac{\partial v_0}{\partial y}\\ \frac{\partial u_0}{\partial y}+\frac{\partial v_0}{\partial x}\end{Bmatrix} \qquad (5)$$

The curvatures are defined by [20]:

$$\begin{Bmatrix}k_x\\ k_y\\ k_{xy}\end{Bmatrix}=\begin{Bmatrix}\frac{\partial}{\partial x}\left(\frac{\partial w_0}{\partial x}\right)\\ \frac{\partial}{\partial y}\left(\frac{\partial w_0}{\partial y}\right)\\ \frac{\partial}{\partial x}\left(\frac{\partial w_0}{\partial y}\right)+\frac{\partial}{\partial y}\left(\frac{\partial w_0}{\partial x}\right)\end{Bmatrix} \qquad (6)$$

The out-of-plane moments are related to the curvatures through the following relations [20]:

$$M_{xx}=D\left(k_x+\upsilon k_y\right)$$
$$M_{yy}=D\left(k_y+\upsilon k_x\right) \qquad (7)$$
$$M_{xy}=\frac{D(1-\upsilon)}{2}k_{xy}$$

where D denotes the plate flexural rigidity and is associated with Young modulus and Poison ratio via

$$D=\frac{Eh^3}{12(1-\upsilon^2)} \qquad (8)$$

The shear force and the total transverse force components are expressed by [20]:

$$Q_x=\frac{\partial M_{xx}}{\partial x}+\frac{\partial M_{xy}}{\partial y}$$
$$Q_y=\frac{\partial M_{yy}}{\partial y}+\frac{\partial M_{xy}}{\partial x} \qquad (9)$$

$$V_x=Q_x+\frac{\partial M_{xy}}{\partial y}$$
$$V_y=Q_y+\frac{\partial M_{xy}}{\partial x} \qquad (10)$$

Some modifications are vital in the aforementioned relations to introduce a refined approach in the differential quadrature element method. The transverse displacement derivatives, according to the following relationships, are firstly considered as [19]:

$$\Psi^x=\frac{\partial w_0}{\partial x}\ ,\ \Psi^y=\frac{\partial w_0}{\partial y} \qquad (11)$$

By changing the degrees of freedom according to rotations of the normal about x and y-axis, the curvature vector can be rewritten as [19]:

$$\begin{Bmatrix} k_x \\ k_y \\ k_{xy} \end{Bmatrix} = \begin{Bmatrix} \dfrac{\partial \Psi^x}{\partial x} \\ \dfrac{\partial \Psi^y}{\partial y} \\ \dfrac{\partial \Psi^y}{\partial x} + \dfrac{\partial \Psi^x}{\partial y} \end{Bmatrix} \tag{12}$$

Also, the out-of-plate moment components are expressed by [19]:

$$\begin{aligned} M_{xx} &= D\left(\frac{\partial \Psi^x}{\partial x} + \upsilon \frac{\partial \Psi^y}{\partial y}\right) \\ M_{yy} &= D\left(\frac{\partial \Psi^y}{\partial y} + \upsilon \frac{\partial \Psi^x}{\partial x}\right) \\ M_{xy} &= \frac{\mathrm{D}(1-\upsilon)}{2}\left(\frac{\partial \Psi^y}{\partial x} + \frac{\partial \Psi^x}{\partial y}\right) \end{aligned} \tag{13}$$

Substituting Eq. (13) into Eq. (1) yields [19]:

$$D\left(\frac{\partial^3 \Psi^x}{\partial x^3} + \frac{\partial^3 \Psi^x}{\partial x \partial y^2} + \frac{\partial^3 \Psi^y}{\partial y \partial x^2} + \frac{\partial^3 \Psi^y}{\partial y^3}\right) = \frac{\partial^2 w_0}{\partial t^2} \tag{14}$$

By substituting Eq. (13) into Eq. (9), the shear force components become [19]

$$\begin{aligned} Q_x &= D\left[\frac{\partial^2 \Psi^x}{\partial x^2} + \left(\frac{1-\upsilon}{2}\right)\frac{\partial^2 \Psi^x}{\partial y^2} + \left(\frac{1+\upsilon}{2}\right)\frac{\partial^2 \Psi^y}{\partial x \partial y}\right] \\ Q_y &= D\left[\frac{\partial^2 \Psi^y}{\partial y^2} + \left(\frac{1-\upsilon}{2}\right)\frac{\partial^2 \Psi^y}{\partial x^2} + \left(\frac{1+\upsilon}{2}\right)\frac{\partial^2 \Psi^x}{\partial x \partial y}\right] \end{aligned} \tag{15}$$

The normal slope, the out-of-plate moment components, and the shear force components on the surface are expressed by Eq. (16) [20]. Where, θ is an angle from the x-axis to the outward normal n-axis.

$$\begin{aligned} M_{nn} &= M_{xx}\cos^2\theta + M_{yy}\sin^2\theta + \\ &\quad 2M_{xy}\sin\theta\cos\theta \\ M_{ns} &= (M_{yy} - M_{xx})\sin\theta\cos\theta + \\ &\quad M_{xy}(\cos^2\theta - \sin^2\theta) \\ Q_n &= Q_x\cos\theta + Q_y\sin\theta \end{aligned} \tag{16}$$

Also, the total transverse force components can be written as follows [20]:

$$V_n = Q_n + \frac{\partial M_{ns}}{\partial s} \tag{17}$$

3- Refined Differential Quadrature Element Method

In this section, the formulation of the refined conventional DQEM is presented by [19]. For this purpose, the equation of motion for thin structure in the form of Eq. (14) is first discretized by using the GDQ method. The key of this method is to determine the derivative of a function with respect to a space variable at a specific point as a weighted linear summation of all the functional values at all other sampling points along with the domain [2] and [4]. Therefore, the first-order partial derivative of a function $f(x)$ with respect to the space variable ξ for the regular domain may be written as:

$$\frac{\partial f}{\partial \xi}\Big|_{x=x_i} = \sum_{k=1}^{N} \bar{A}_{ik}^{x} f_{kj} \tag{18}$$

where N is the number of sampling points in the domain and $A_{ik}^{(r)}$ is the weighting coefficients to be defined as follows [4]:

$$\bar{A}_{ik}^{x} = \begin{cases} \dfrac{\prod(\xi_i)}{(\xi_i - \xi_k)\prod(\xi_k)} & i \neq j \\ -\displaystyle\sum_{v=1, v\neq i}^{M} A_{iv}^{(1)} & i = j \end{cases} \tag{19}$$

A well-known method of defining these points is to use Chebyshev-Gauss-Lobatto point distribution given by Shu [2-3] as:

$$\xi_i = -\cos\frac{(i-1)}{(\mathrm{N}-1)}\pi, \quad i = 1, 2, \ldots, N \tag{20}$$

The first-order partial derivative of a function $f(x)$ can be expressed in x-y coordinate by geometric mapping presented by Eq. (21) [21].

$$\begin{aligned} \frac{\partial f}{\partial x} &= \frac{1}{|J|}\left(\frac{\partial y}{\partial \eta}.\frac{\partial f}{\partial \xi} - \frac{\partial y}{\partial \xi}.\frac{\partial f}{\partial \eta}\right) \\ \frac{\partial f}{\partial y} &= \frac{1}{|J|}\left(\frac{\partial x}{\partial \xi}.\frac{\partial f}{\partial \eta} - \frac{\partial x}{\partial \eta}.\frac{\partial f}{\partial \xi}\right) \end{aligned} \tag{21}$$

where $\left|J\right|$ is Jacobean expressed by Eq. (22).

$$\left|J\right| = \frac{\partial x}{\partial \xi}\cdot\frac{\partial y}{\partial \eta} - \frac{\partial y}{\partial \xi}\cdot\frac{\partial x}{\partial \eta} \tag{22}$$

By substituting Eq. (18) into Eq. (21), the first-order partial derivatives of a function *f(x)* in *x-y* become [21]:

$$\begin{aligned}&\left(\frac{\partial f}{\partial x}\right)_{ij} = \frac{1}{\left|J\right|_{ij}}\times\\&\left[\left(\frac{\partial y}{\partial \eta}\right)_{ij}\cdot\left(\sum_{k=1}^{N}\bar{A}_{ik}^{x} f_{kj}\right) - \left(\frac{\partial y}{\partial \xi}\right)_{ij}\cdot\left(\sum_{m=1}^{M}\bar{A}_{jm}^{y} f_{im}\right)\right]\\&\left(\frac{\partial f}{\partial y}\right)_{ij} = \frac{1}{\left|J\right|_{ij}}\times\\&\left[\left(\frac{\partial x}{\partial \xi}\right)_{ij}\cdot\left(\sum_{m=1}^{M}\bar{A}_{jm}^{y} f_{im}\right) - \left(\frac{\partial y}{\partial \xi}\right)_{ij}\cdot\left(\sum_{k=1}^{N}\bar{A}_{ik}^{x} f_{kj}\right)\right]\end{aligned} \tag{23}$$

Eq. (23) can be rewritten by Eq. (24).

$$\begin{aligned}&\left.\frac{\partial f}{\partial x}\right|_{n} = \sum_{k=1}^{N\times M} A_{nk}^{x}.f_k\\&\left.\frac{\partial f}{\partial x}\right|_{n} = \sum_{k=1}^{N\times M} A_{nk}^{y}.f_k\\&where: \quad n=(\mathrm{i}-1).N+j \quad ; \quad f_n = f_{ij}\end{aligned} \tag{24}$$

$A^{(\mathrm{r})}$ and $A^{(\mathrm{rs})}$ are defined by Eq. (25). for the *r*-th order partial derivative [21].

$$\begin{aligned}&\left[A^{(\mathrm{r})\mathrm{x}}\right] = \left[A^{(1)\mathrm{x}}\right].\left[A^{(\mathrm{r-1})\mathrm{x}}\right]; \quad r=2,3,...\\&\left[A^{(\mathrm{rs})\mathrm{xy}}\right] = \left[A^{(\mathrm{r})\mathrm{x}}\right].\left[A^{(\mathrm{s})\mathrm{y}}\right]; \quad r,s=1,2,...\end{aligned} \tag{25}$$

It should be noted that the weighting coefficients are only dependent on the derivative order and on the number and distribution of sampling points along with the domain. By defining the degrees of freedom slope at the edge of an element and the transverse displacement in all domains; $\frac{\partial \psi^x}{\partial \xi}$ $\frac{\partial^2 \psi^x}{\partial \xi \partial \eta}$ ، $\frac{\partial \psi^y}{\partial \eta}$ ، and $\frac{\partial^2 \psi^y}{\partial \xi \partial \eta}$ can be expressed in the DQ discretization form as:

$$\begin{aligned}&\frac{\partial \Psi^x}{\partial x} = \sum_{k_1=1}^{N\times M} A_{nk_1}^{x}\Psi_{k_1}^{x} =\\&A_{na_1}^{x}\Psi_{a_1}^{x} + A_{na_2}^{x}\Psi_{a_2}^{x} + \sum_{k_1=c}^{d}\sum_{k_2=1}^{N\times M} A_{nk_1}^{x}A_{k_1k_2}^{x} w_{k_2}\\&\frac{\partial \Psi^y}{\partial y} = \sum_{k_3=1}^{N\times M} A_{nk_3}^{y}\Psi_{n}^{y} =\\&A_{nb_1}^{y}\Psi_{b_1}^{y} + A_{nb_2}^{y}\Psi_{b_2}^{y} + \sum_{k_3=e}^{f}\sum_{k_4=1}^{N\times M} A_{nk_3}^{y}A_{k_3k_4}^{y} w_{k_4}\\&\frac{\partial^2 \Psi^x}{\partial x\,\partial y} = \sum_{k_1=1}^{N\times M} B_{nk_1}^{xy}\Psi_{k_1}^{x} =\\&B_{na_1}^{xy}\Psi_{a_1}^{x} + B_{na_2}^{xy}\Psi_{a_2}^{x} + \sum_{k_1=c}^{d}\sum_{k_2=1}^{N\times M} B_{nk_1}^{xy}A_{k_1k_2}^{x} w_{k_2}\\&\frac{\partial^2 \Psi^y}{\partial x\,\partial y} = \sum_{k_3=1}^{N\times M} A_{nk_3}^{xy}\Psi_{n}^{y} =\\&B_{nb_1}^{xy}\Psi_{b_1}^{y} + A_{nb_2}^{xy}\Psi_{b_2}^{y} + \sum_{k_3=e}^{f}\sum_{k_4=1}^{N\times M} B_{nk_3}^{xy}A_{k_3k_4}^{y} w_{k_4}\end{aligned} \tag{26}$$

$$\begin{aligned}&where:\\&a_1 = j \quad ,a_2 = \left[(\mathrm{N}-1)\times\mathrm{N}\right]+\mathrm{j} \quad ,\\&n = \left[(i-1)\times\mathrm{N}\right]+\mathrm{j} \quad ,\\&c = \left[(k_1-1)\times\mathrm{N}\right]+\mathrm{j};\ \mathrm{k}_1 \geq 2\\&c = \left[(k_1-1)\times\mathrm{N}\right]+\mathrm{j};\ k_1 \leq N-1\\&b_1 = \left[(i-1)\times\mathrm{N}\right]+1 \quad ,\\&b_2 = \left[(i-1)\times\mathrm{N}\right]+M \quad ,\\&\mathrm{e} = \left[(i-1)\times\mathrm{N}\right]+k_3;\ \mathrm{k}_3 \geq 2\\&c = \left[(i-1)\times\mathrm{N}\right]+k_3;\ k_3 \leq M-1\end{aligned}$$

Where N and M denote the number of computational/ sampling points in x and y-direction, respectively. In the above equations, it can be seen that there are two and three degrees of freedom at the edges and the corner points of a computational domain (element) with an arbitrary shape. [19].

Substituting the partial derivatives in Eq. (16), in a similar manner to Eq. (14), the following equation will be achieved.

$$\begin{aligned}&\left(C^{x}_{na_1}\Psi^{x}_{a_1}+C^{x}_{na_2}\Psi^{x}_{a_2}+\sum_{k_1=c}^{d}\sum_{k_2=1}^{N\times M}C^{x}_{nk_1}A^{x}_{k_1k_2}w_{k_2}\right)+\\&\left(C^{y}_{nb_1}\Psi^{y}_{b_1}+C^{y}_{nb_2}\Psi^{y}_{b_2}+\sum_{k_3=e}^{f}\sum_{k_4=1}^{N\times M}C^{x}_{nk_3}A^{y}_{k_3k_4}w_{k_4}\right)\\&+\left(C^{xy}_{na_1}\Psi^{x}_{a_1}+C^{xy}_{na_2}\Psi^{x}_{a_2}+\sum_{k_1=c}^{d}\sum_{k_2=1}^{N\times M}C^{xy}_{nk_1}A^{x}_{k_1k_2}w_{k_2}\right)+\\&\left(C^{xy}_{nb_1}\Psi^{y}_{b_1}+C^{xy}_{nb_2}\Psi^{y}_{b_2}+\sum_{k_3=e}^{f}\sum_{k_4=1}^{N\times M}C^{xy}_{nk_3}A^{y}_{k_3k_4}w_{k_4}\right)=\Omega^2 w_{ij}\\&\quad for\;\;2\le i\le N-1\;\;and\;\;2\le j\le M-1\end{aligned}\tag{27}$$

where C^x and B^x are the weighting coefficients correspond to the third and second-order partial derivative in the *x*-direction and C^y , and B^y are those in the *y*-direction, similarly.

$$\begin{aligned}M_{xx}&=D\left(A^{x}_{na_1}\Psi^{x}_{a_1}+A^{x}_{na_2}\Psi^{x}_{a_2}+\sum_{k_1=c}^{d}\sum_{k_2=1}^{N\times M}A^{x}_{nk_1}A^{x}_{k_1k_2}w_{k_2}\right)+\\&D\upsilon\left(A^{y}_{nb_1}\Psi^{y}_{b_1}+A^{y}_{nb_2}\Psi^{y}_{b_2}+\sum_{k_3=e}^{f}\sum_{k_4=1}^{N\times M}A^{y}_{nk_3}A^{y}_{k_3k_4}w_{k_4}\right)\\M_{yy}&=D\upsilon\left(A^{y}_{nb_1}\Psi^{y}_{b_1}+A^{y}_{nb_2}\Psi^{y}_{b_2}+\sum_{k_3=e}^{f}\sum_{k_4=1}^{N\times M}A^{y}_{nk_3}A^{y}_{k_3k_4}w_{k_4}\right)+\\&D\left(A^{x}_{na_1}\Psi^{x}_{a_1}+A^{x}_{na_2}\Psi^{x}_{a_2}+\sum_{k_1=c}^{d}\sum_{k_2=1}^{N\times M}A^{x}_{nk_1}A^{x}_{k_1k_2}w_{k_2}\right)\\M_{xy}&=\frac{D(1-\nu)}{2}\left(A^{x}_{nb_1}\Psi^{y}_{b_1}+A^{x}_{nb_2}\Psi^{y}_{b_2}+\sum_{k_3=e}^{f}\sum_{k_4=1}^{N\times M}A^{x}_{nk_3}A^{y}_{k_3k_4}w_{k_4}\right)+\\&\frac{D(1-\nu)}{2}\left(A^{y}_{na_1}\Psi^{x}_{a_1}+A^{y}_{na_2}\Psi^{x}_{a_2}+\sum_{k_1=c}^{d}\sum_{k_2=1}^{N\times M}A^{y}_{nk_1}A^{x}_{k_1k_2}w_{k_2}\right)\\\frac{Q_x}{D}&=\left(B^{x}_{na_1}\Psi^{x}_{a_1}+B^{x}_{na_2}\Psi^{x}_{a_2}+\sum_{k_1=c}^{d}\sum_{k_2=1}^{N\times M}B^{x}_{nk_1}A^{x}_{k_1k_2}w_{k_2}\right)+\\&\frac{(1+\nu)}{2}\left(B^{xy}_{nb_1}\Psi^{y}_{b_1}+B^{xy}_{nb_2}\Psi^{y}_{b_2}+\sum_{k_3=e}^{f}\sum_{k_4=1}^{N\times M}B^{xy}_{nk_3}A^{y}_{k_3k_4}w_{k_4}\right)\\&+\frac{(1-\nu)}{2}\left(B^{y}_{na_1}\Psi^{x}_{a_1}+B^{y}_{na_2}\Psi^{x}_{a_2}+\sum_{k_1=c}^{d}\sum_{k_2=1}^{N\times M}B^{y}_{nk_1}A^{x}_{k_1k_2}w_{k_2}\right)\\\frac{Q_y}{D}&=\left(B^{y}_{nb_1}\Psi^{y}_{b_1}+B^{y}_{nb_2}\Psi^{y}_{b_2}+\sum_{k_3=e}^{f}\sum_{k_4=1}^{N\times M}B^{y}_{nk_3}A^{y}_{k_3k_4}w_{k_4}\right)+\\&\left(\frac{1+\nu}{2}\right)\left(B^{xy}_{na_1}\Psi^{x}_{a_1}+B^{xy}_{na_2}\Psi^{x}_{a_2}+\sum_{k_1=c}^{d}\sum_{k_2=1}^{N\times M}B^{xy}_{nk_1}A^{x}_{k_1k_2}w_{k_2}\right)+\\&\frac{(1-\upsilon)}{2}\left(B^{x}_{nb_1}\Psi^{y}_{b_1}+B^{x}_{nb_2}\Psi^{y}_{b_2}+\sum_{k_3=e}^{f}\sum_{k_4=1}^{N\times M}B^{x}_{nk_3}A^{y}_{k_3k_4}w_{k_4}\right)\end{aligned}\tag{28}$$

4- Boundary Conditions

In this section, different conventional boundary conditions are introduced, and their discretized forms are presented.

4- 1- Clamped boundary condition

At edges $x=0$ or $x=a$: $w=0$ and $\Psi^n=0$.

These equations can be written in DQ form as

$$\begin{aligned}&\text{At}\quad x=0,\quad w_{n_1}=0\\&\text{and}\quad \Psi^n_{n_1}=0\quad where\quad n_1=j\\&\text{At}\quad x=a,\quad w_{n_2}=0\\&\text{and}\quad \Psi^n_{n_2}=0\quad where\quad n_2=\left[(\mathrm{N}-1)\times\mathrm{N}\right]+j\end{aligned}\tag{29}$$

At edges $y=0$ or $y=b$: $w=0$ and $\Psi^n=0$.

These equations can be shown in the discretized form similar to the previous items.

$$\begin{aligned}&\text{At}\quad y=0,\quad w_{n_1}=0\\&\text{and}\quad \Psi^n_{n_1}=0\\&where\quad n_1=\left[(\mathrm{i}-1)\times\mathrm{N}\right]+1\\&\text{At}\quad y=b,\quad w_{n_2}=0\\&\text{and}\quad \Psi^n_{n_2}=0\\&where\quad n_2=\left[(\mathrm{i}-1)\times\mathrm{N}\right]+M\end{aligned}\tag{30}$$

4- 2- Simply support boundary conditions

At edges $x=0$ or $x=a$: $w=0$ and $M^{nn}=0$.

These equations can be written in DQ form as

$$\begin{aligned}&\text{At}\quad x=0,\quad w_{n_1}=0\\&\text{and}\quad M^{nn}_{n_1}=0\quad where\quad n_1=j\\&\text{At}\quad x=a,\quad w_{n_2}=0\\&\text{and}\quad M^{nn}_{n_2}=0\\&where\quad n_2=\left[(\mathrm{N}-1)\times\mathrm{N}\right]+j\end{aligned}\tag{31}$$

At $y=0$ or $y=b$: $w=0$ and $M^{nn}=0$.

These equations can be expressed in a discretized form similar to the prior items.

$$\begin{aligned}&\text{At}\quad y=0,\quad w_{n_1}=0\\&\text{and}\quad M^{nn}_{n_1}=0\\&\textit{where}\quad n_1=[(\mathrm{i}-1)\times \mathrm{N}]+1\\&\text{At}\quad y=b,\quad w_{n_2}=0\\&\text{and}\quad M^{nn}_{n_2}=0\\&\textit{where}\quad n_2=[(\mathrm{i}-1)\times \mathrm{N}]+M\end{aligned} \tag{32}$$

4- 3- Free boundary conditions

At $x=0$ or $x=a$: $V^{nn}=0$ and $M^{nn}=0$.

These equations can be written in DQ form as

$$\begin{aligned}&\text{At}\quad x=0,\quad V^{nn}_{n_1}=0\\&\text{and}\quad M^{nn}_{n_1}=0\\&\textit{where}\quad n_1=j\\&\text{At}\quad x=a,\quad V^{nn}_{n_2}=0\\&\text{and}\quad M^{nn}_{n_2}=0\\&\textit{where}\quad n_2=[(\mathrm{N}-1)\times \mathrm{N}]+j\end{aligned} \tag{33}$$

At edges $y=0$ or $y=b$: $V^{nn}=0$ and $M^{nn}=0$.

$$\begin{aligned}&\text{At}\quad y=0,\quad V^{nn}_{n_1}=0\\&\text{and}\quad M^{nn}_{n_1}=0\\&\textit{where}\quad n_1=[(i-1)\times \mathrm{N}]+1\\&\text{At}\quad y=b,\quad V^{nn}_{n_2}=0\\&\text{and}\quad M^{nn}_{n_2}=0\\&\textit{where}\quad n_2=[(i-1)\times \mathrm{N}]+M\end{aligned} \tag{34}$$

4- 4- The boundary conditions of corner point

If corner points have a combination of simply support and clamped boundary conditions simultaneously or have an identical specific boundary condition (clamped or simply support), the boundary conditions at this point can be expressed by:

$$w=0\ ,\ \psi^x=0\ ,\ \psi^y=0 \tag{35}$$

The boundary conditions of a corner on the intersection of two adjacent free edges are

$$\begin{aligned}&M^{nn}=0\ ,\ M^{ss}=0\ ,\\&S=M^{ns}\big|_{edge\,1}-M^{ns}\big|_{edge\,2}=0\end{aligned} \tag{36}$$

4- 5- The connection between elements

It should be noted that the physical connection between the adjacent elements is provided by the compatibility conditions, including continuity of transverse displacement, rotation, bending moments, and shear forces. So, the continuity conditions can be expressed in the normal direction as follows:

$$\begin{aligned}&w\big|_{edge\,1}-w\big|_{edge\,2}=0\ ,\\&\Psi^n\big|_{edge\,1}-\Psi^n\big|_{edge\,2}=0\\&M^{nn}\big|_{edge\,1}-M^{nn}\big|_{edge\,2}=0,\\&V^{nn}\big|_{edge\,1}-V^{nn}\big|_{edge\,2}=0\end{aligned} \tag{37}$$

5- Solution Methodology

The set of governing equations can be expressed by

$$[M]\{\ddot{\delta}\}+[K]\{\delta\}=\{0\} \tag{38}$$

With assuming $\{\delta\}=\{\delta\}e^{i\Omega t}$ Eq. (38) can be written by

$$\left([K]-\Omega^2[M]\right)\{\delta\}=0 \tag{39}$$

According to the static condensation concept, the combination of the aforementioned discretized governing equations and the associated boundary condition equations can be represented by a system of linear equations through an assembling procedure such that the continuity conditions between adjacent DQ elements are satisfied (see more details in Ref. [16]).

$$\begin{bmatrix}K_{BB} & K_{BD}\\ K_{DB} & K_{DD}\end{bmatrix}\begin{bmatrix}\delta_B\\ \delta_D\end{bmatrix}-\Omega^2\begin{bmatrix}0\\ \delta_D\end{bmatrix}=\begin{bmatrix}0\\ 0\end{bmatrix} \tag{40}$$

where the subscripts B and D denote the boundary and interior points along with the domain, respectively. K_{BB}, K_{BD}, K_{DB} and K_{DD} imply the influence coefficients

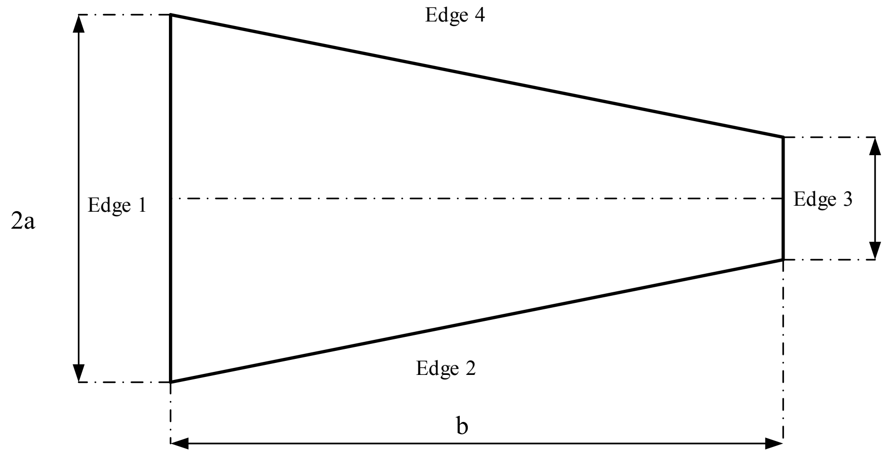

Fig. 1. A symmetric trapezoidal thin plate.

appeared in the discretized equations. δ_B is the degree of freedom vector including transverse displacements and slope states which are considered on the boundaries of the domain and defined by:

$$\delta_B = \left\{ \{w\}_B \quad \{\psi^x\}_B \quad \{\psi^y\}_B \right\}^T \tag{41}$$

Also, δ_D is the degree freedom vector including transverse displacement of the interior points along the domain and defined by:

$$\delta_D = \{w\}_D \tag{42}$$

Computing δ_D from the first row of Eq. (40) and substituting it into the second-row results in the following relation.

$$K\delta_D = \Omega^2 \delta_D \tag{43}$$

where

$$K = K_{DD} - K_{DB} K_{BB}^{-1} K_{BD} \tag{44}$$

The eigen-frequencies of Eq. (43) can be determined through a standard eigenvalue solver.

6- Results and Discussions

In this section, the free vibration analyses of three thin plate test cases are conducted by the developed numerical tool.

6- 1- Free vibration of a single domain with arbitrary shape

In order to evaluate the accuracy and fidelity of the present approach, free vibration analysis of a trapezoidal plate with several different boundary conditions that are shown in Fig. 1 is carried out. Table 1 presents the convergence behavior of the first eight non-dimensionalized natural frequencies of the trapezoidal plate under the fully clamped boundary condition with increasing sampling points in the domain. In order to perform the convergence study of the present method, different numbers of sampling points have been considered. A good monotonic convergence behavior could be noticed, and a 24×24 sampling point is found to provide sufficiently accurate results.

Table 2 shows the first five non-dimensional natural frequencies of symmetric trapezoidal thin plate with several boundary conditions in comparison with Ref. [21] that is obtained by a combination of conventional GDQM (CGDQM) with mapping method for a simple domain that this method has not capable of applying free boundary and continuity conditions. The presented results in Table 2 show an excellent accuracy in comparison with those reported by Ref. [21].

In the next study, the free vibration analysis of the skew plate with different boundary conditions is examined. Table 3 shows the non-dimensional natural frequencies of this test

Table 1. Non-dimensional natural frequencies ($\Omega=\omega(a/\pi)^2\sqrt{\rho h/D}$) of a symmetric trapezoidal thin plate under clamped boundary conditions with $b/a=3$ and $a/c=2.5$

	Mode sequence					
Method	1	2	3	4	5	6
Present (9 × 9)	10.4334	15.4107	20.7297	23.007	23.0346	23.8607
Present (10 × 10)	10.4236	15.4867	20.4276	23.7694	24.4243	32.2927
Present (11 × 11)	10.4296	15.5699	21.3632	23.8928	24.3680	30.3402
Present (12 × 12)	10.4274	15.5668	21.4238	23.9092	27.8697	27.8697
Present (13 × 13)	10.4288	15.5643	21.4806	23.9050	29.4442	29.4442
Present (14 × 14)	10.4280	15.5640	21.4747	23.9052	28.8236	32.5396
Present (15 × 15)	10.4280	15.5640	21.4747	23.9052	28.8236	32.5396
Present (16 × 16)	10.4273	15.5633	21.4766	23.9083	28.8409	32.5414
Present (17 × 17)	10.4276	15.5637	21.4761	23.9054	28.8435	32.5401
Present (18 × 18)	10.4273	15.5633	21.4763	23.9069	28.8406	32.5412
Present (19 × 19)	10.4274	15.5635	21.4761	23.9054	28.8420	32.5401
Present (20 × 20)	10.4273	15.5634	21.4762	23.9061	28.8411	32.5407
Present (21 × 21)	10.4274	15.5634	21.4761	23.9054	28.8418	32.5401
Present (22 × 22)	10.4273	15.5634	21.4762	23.9057	28.8414	32.5405
Present (23 × 23)	10.4273	15.5634	21.4761	23.9054	28.8417	32.5401
Present (24 × 24)	10.4273	15.5634	21.4762	23.9055	28.8415	32.5403

Table 2. Non-dimensional natural frequencies ($\Omega=\omega(a/\pi)^2\sqrt{\rho h/D}$) of a symmetric trapezoidal thin plate under clamped boundary conditions with $b/a=3$ and $a/c=2.5$

		Mode sequence				
Boundary condition	Method	1	2	3	4	5
C-C-C-C	Present	10.427	15.563	21.476	23.905	28.841
	Ref.[21]	10.427	15.563	21.476	23.905	28.842
S-S-S-S	Present	5.389	9.423	14.688	15.910	21.690
	Ref.[21]	5.389	9.422	14.685	15.908	21.689
S-C-S-C	Present	9.443	14.386	19.897	22.4694	26.331
	Ref.[21]	9.443	14.386	19.897	22.472	26.331

case study in comparison with Refs. [22-24] that are obtained by finite element method, generalized differential quadrature method based on first-order deformation theory, and Ritz method, respectively. The achieved results show high accuracy as well as other references, especially in implementing free boundary conditions. The DQM, as the known form, is not able to solve the derived partial differential equations of classical theory for the thin plate with arbitrary geometry, including free boundary conditions. This table shows that the problem of applying free boundary conditions is solved.

To evaluate the accuracy and fidelity of the present approach for connection among several elements, free vibration analysis of a square plate composed of two subdomains under the clamp and support boundary conditions, which are shown in Fig. 3 is investigated.

Table 4 shows the natural frequencies for a square plate

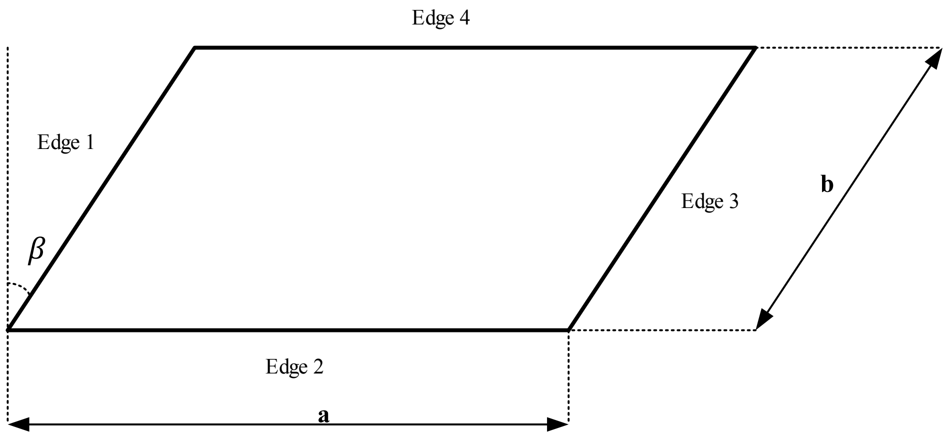

Fig. 2. Schematic figure of the skew plate.

Table 3. Non-dimensional natural frequencies ($\Omega = \omega(a/\pi)^2 \sqrt{\rho h/D}$) of a skew plate

			Mode sequence				
Boundary condition	**Method**	β	**1**	**2**	**3**	**4**	**5**
C-C-C-C	Present	60	12.3247	18.0069	23.4808	29.5373	30.8788
	Ref.[22]		12.3399	18.0057	23.4956	29.5649	30.9447
S-S-S-S	Present	15	2.1130	4.8842	5.6845	8.0090	10.5374
	Ref.[23]		2.1144	4.8842	5.6846	8.0085	10.5372
S-C-S-C	Present	30	3.7440	6.5112	9.4198	10.2110	13.9495
	Ref.[22]		3.7451	6.5119	9.4233	10.2112	13.9530
C-F-C-F	Present	45	3.6856	3.8447	6.2487	8.7815	10.3478
	Ref.[23]		3.6852	3.8432	6.2509	8.7740	10.3352
S-F-S-F	Present	60	2.5700	2.7109	5.5671	7.3968	10.1871
	Ref.[22]		2.5810	2.7249	5.4567	7.3786	10.1551
F-F-F-F	Present	0	1.3645	1.9855	2.4591	3.5261	3.5261
	Ref.[24]		1.3667	2.005	2.4755	3.4736	3.4736

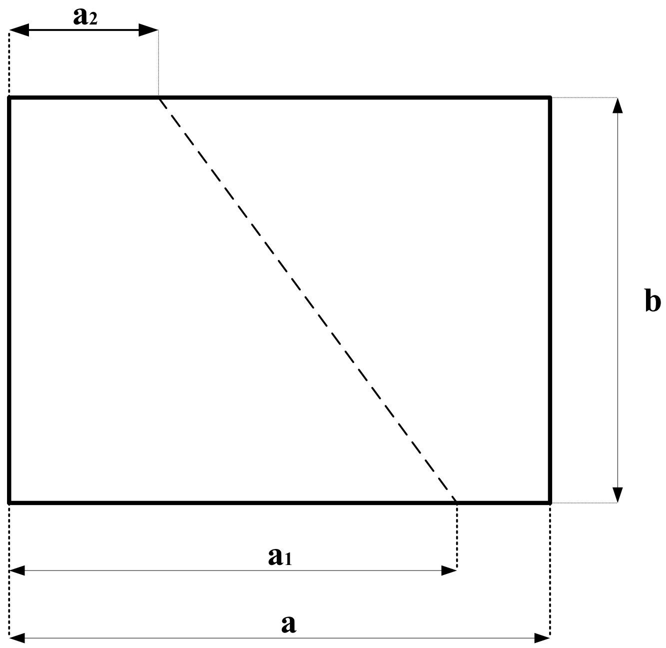

Fig. 3. A rectangular thin plate consists of two subdomains with $a_1/a = 0.75$ **and** $a_2/a = 0.25$ **.**

Table 4. Non-dimensional natural frequencies ($\Omega = \omega a^2 \sqrt{\rho h/D}$**) of a square plate consist of two subdomains**

		Mode sequence				
Boundary condition	**Method**	**1**	**2**	**3**	**4**	**5**
C-C-C-C	Present	35.9853	73.3939	73.3939	108.215	131.580
	CDQM [16]	35.9852	73.3939	73.3939	108.217	131.579
	Ref.[24]	35.992	73.413	73.413	108.270	131.640
`S-S-S-S	Present	19.7392	49.3480	49.3480	78.9568	98.6960
	CDQM [16]	19.7392	49.3480	49.3480	78.9568	98.6960
	Ref.[24]	19.7392	49.3480	49.3480	78.9568	98.6960

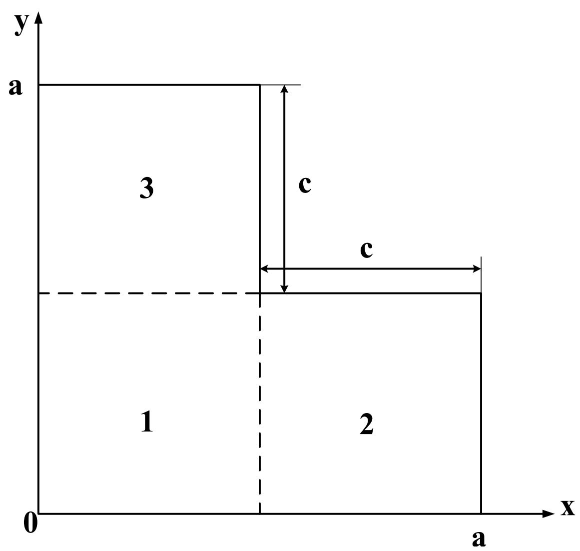

Fig. 4. The L-shaped thin plate with cut out.

consisting of two subdomains, and the connection between subdomains has been established by continuity conditions. The results have been presented by 16×16 sampling points in each subdomain. The results have been compared by [16] which are presented based on Conventional DQM for a single domain with 16×16 sampling points. The convergence of the present method needs more grid points than ordinary DQM, but the high accuracy has made it convenient to use the presented approach for solving thin plates with an arbitrary shape or consist of multi-domain.

6- 2- The free vibration of an L-Shape thin plate

In this section, the free vibration analysis of a simply supported L-shaped thin plate with equal sides is conducted. In order to apply the present approach (GDQEM) for solving this problem, the plate is divided into three subdomains, as shown in Fig. 4.

The results consist of the first four non-dimensional natural frequencies along with those reported in Ref. [25] are presented in Fig. 5. Also, the effect of the cutout aspect ratio (c/a) on the natural frequency has been studied and depicted in this figure. It should be noted that a sampling point distribution including 22×22 grid points in each subdomain has been considered to achieve an acceptable convergence. As it is evident, there is an excellent correlation between the results of the present method and Ref. [25].

The first four shape modes of this thin plate structure have been presented in Fig. 6.

6- 3- The free vibration of a square thin plate with mixed boundary conditions

In this section, the results of free vibration analysis of a square plate with mixed boundary conditions are presented by using the present method. Fig. 7 shows a square plate with simply supported, free, and clamped boundary conditions at the same edges. For this purpose, the plate is divided into six subdomains (as shown in Fig. 7), and a sampling point distribution including 22×22 grid points in each subdomain is considered.

The first four non-dimensional natural frequencies of the first case, corresponding to Fig. 7, are presented in Fig. 8. The obtained results are in good agreement with those of Ref. [27]. It should be noted that the results of Ref. [27] were obtained by applying DQEM to analyze the above problems based on the first-order shear deformation theory.

7- Conclusions

In this study, the combination of geometric mapping with a refined approach in the generalized differential quadrature element method has been proposed to provide the free vibration analysis of thin plate structures with complex geometry or boundary conditions. The main idea of this approach is to refine the GDQ formulation based on the classical plate theory by incorporating an additional degree of freedom. To validate the present approach, free vibration analyses of some different test cases, including symmetric trapezoidal thin plate, skew thin plate, L-shape thin plates, and square thin plates with mixed boundary conditions, have been performed. The evaluation of the obtained results clarifies the accuracy and fidelity of the present method. However, it was found that the convergence of the present method needs more grid points than ordinary DQM. However, using the developed formulation, one can overcome the difficulties in applying different types of boundary and the simulation of geometry with arbitrary shape in the computational domain based on classical theory.

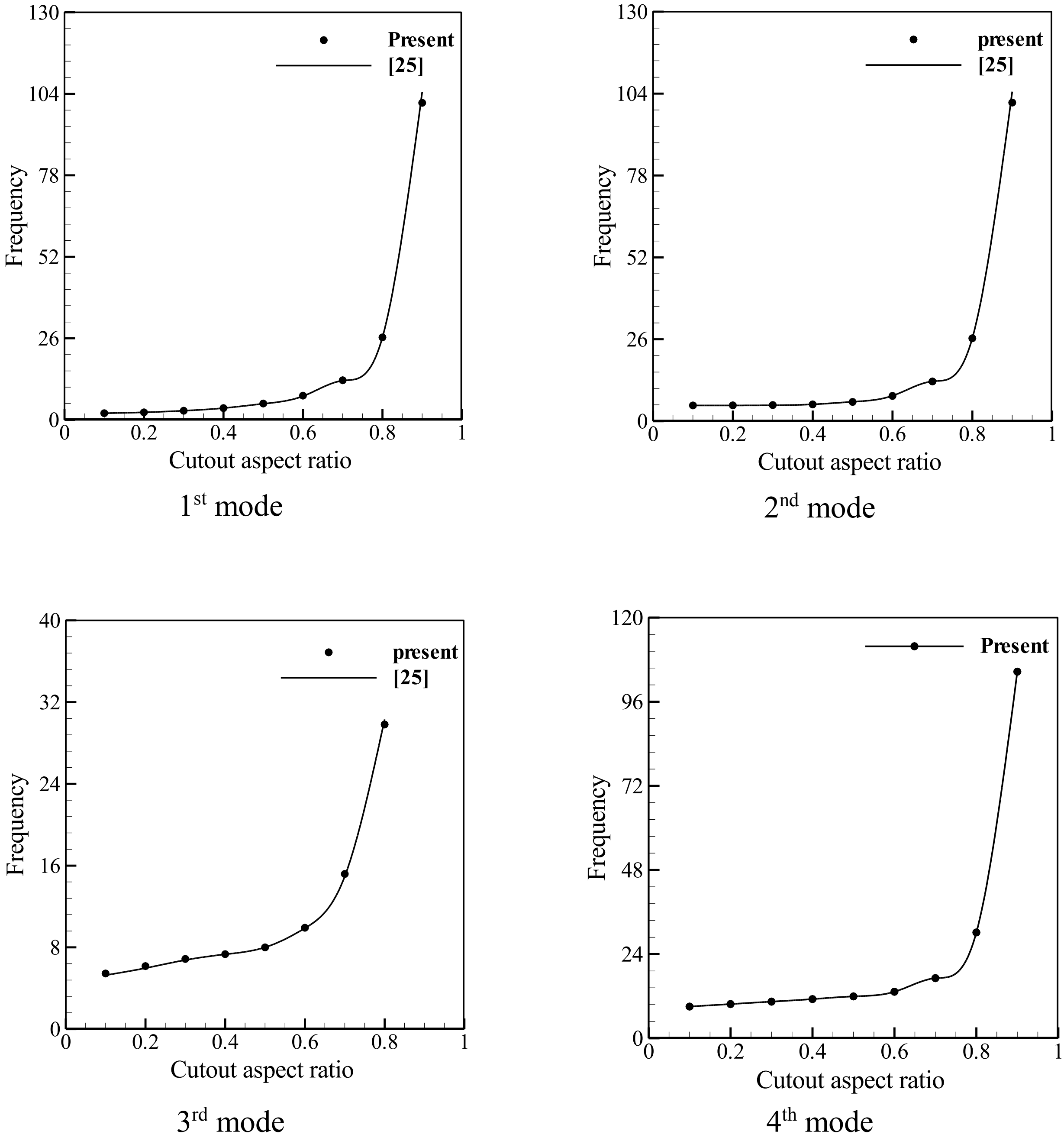

Fig. 5. Variation of the natural frequencies of the simply supported L-Shaped plate with a cut-out aspect ratio

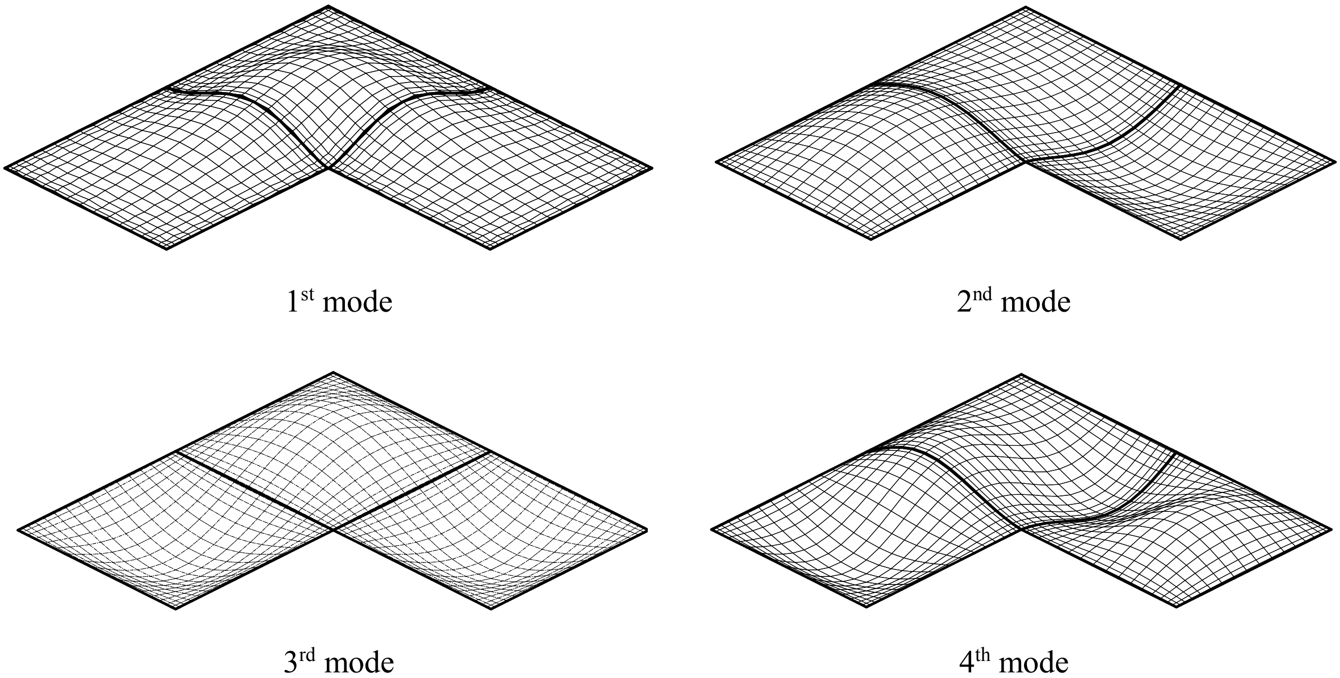

Fig. 6. The first four mode shapes of the simply supported L-Shaped thin plate

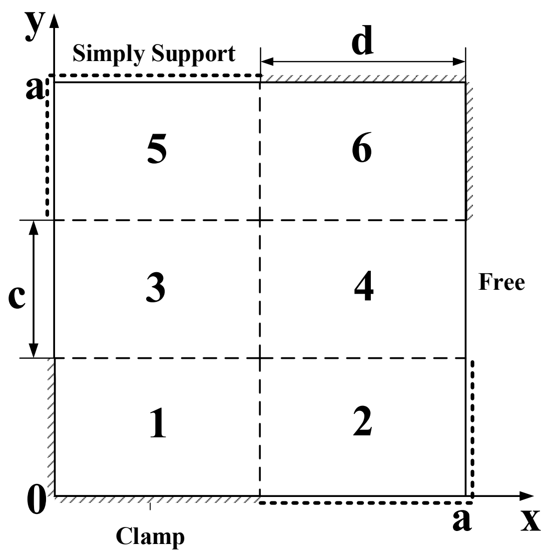

Fig. 7. a square plate with simply supported, free, and clamped boundary conditions.

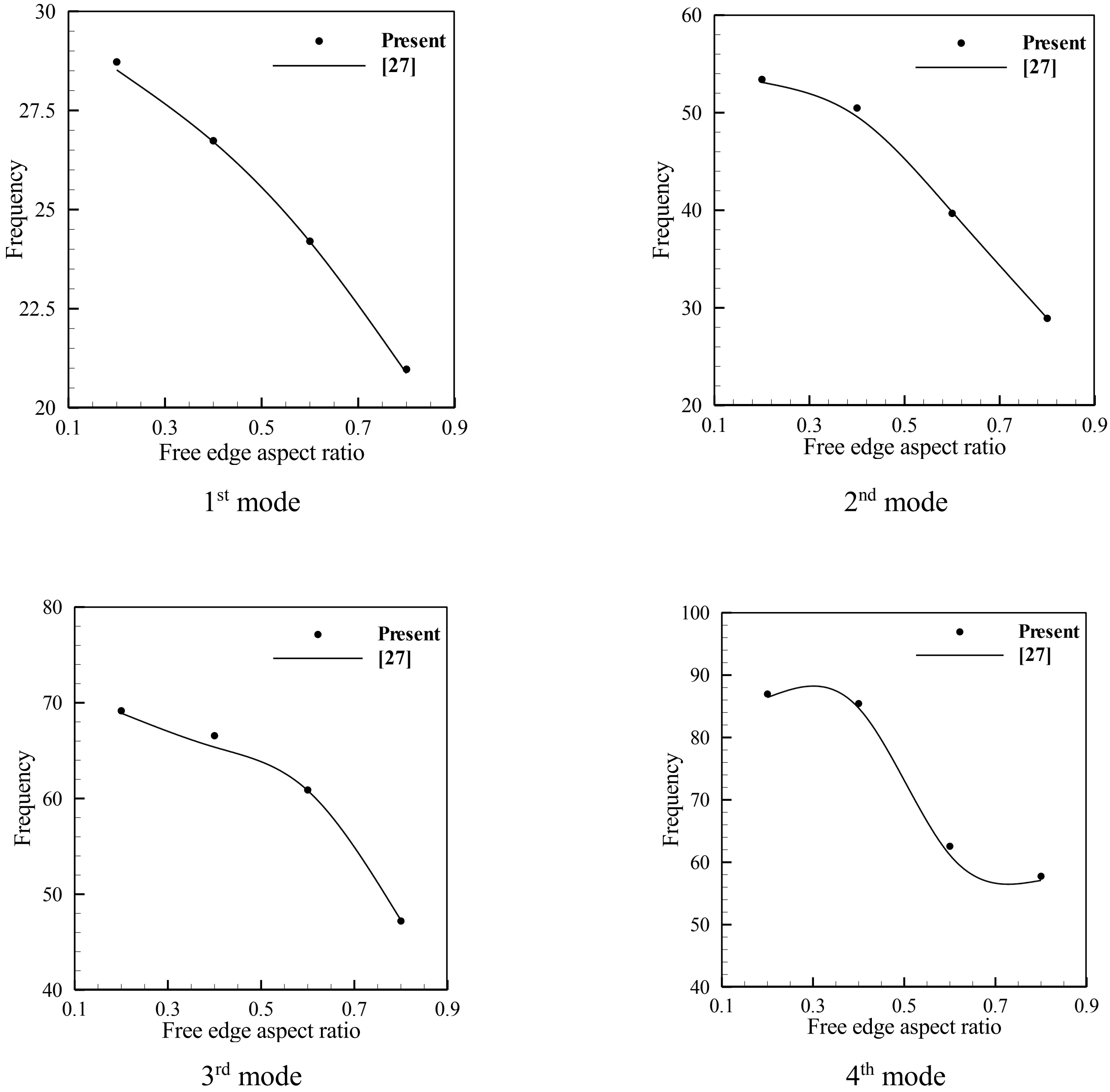

Fig. 8. Variation of the natural frequencies of the simply supported L-Shaped plate with a cut-out aspect ratio

Reference

[1] R. Bellman, J. Casti, Differential quadrature and long-term integration, Journal of Mathematical Analysis and Applications, 34(2) (1971) 235-238.

[2] C. Shu, Differential quadrature and its application in engineering, Springer Science & Business Media, 2012.

[3] F. Tornabene, N. Fantuzzi, F. Ubertini, E. Viola, Strong formulation finite element method based on differential quadrature: a survey, Applied Mechanics Reviews, 67(2) (2015).

[4] C. Shu, B.E. Richards, Application of generalized differential quadrature to solve two-dimensional incompressible Navier-Stokes equations, International Journal for Numerical Methods in Fluids, 15(7) (1992) 791-798.

[5] M. Javadi, V. Khalafi, Flutter reliability analysis of laminated composite plates, Amirkabir Journal of Mechanical Engineering, 53(6 (Special Issue)) (2021) 10-10.

[6] V. Khalafi, H. Shahverdi, S. Noori, Nonlinear Aerothermoelastic Analysis of Functionally Graded Rectangular Plates Subjected to Hypersonic Airflow Loadings, AUT Journal of Mechanical Engineering, 2(2) (2018) 217-232.

[7] X. Wang, Z. Yuan, Buckling analysis of isotropic skew plates under general in-plane loads by the modified differential quadrature method, Applied Mathematical Modelling, 56 (2018) 83-95.

[8] A.G. Striz, C. Weilong, C.W. Bert, Static analysis of structures by the quadrature element method (QEM), International Journal of Solids and Structures, 31(20) (1994) 2807-2818.

[9] L. Ke, Y. Wang, J. Yang, S. Kitipornchai, F. Alam, Nonlinear vibration of edged cracked FGM beams using differential quadrature method, Science China Physics, Mechanics and Astronomy, 55(11) (2012) 2114-2121.

[10] K. Torabi, H. Afshari, F.H. Aboutalebi, A DQEM for transverse vibration analysis of multiple cracked non-uniform Timoshenko beams with general boundary conditions, Computers & Mathematics with Applications, 67(3) (2014) 527-541.

[11] F.-L. Liu, K. Liew, Vibration analysis of discontinuous Mindlin plates by differential quadrature element method, (1999).

[12] F.-L. Liu, K. Liew, Differential quadrature element method: a new approach for free vibration analysis of polar Mindlin plates having discontinuities, Computer Methods in Applied Mechanics and Engineering, 179(3-4) (1999) 407-423.

[13] N. Fantuzzi, F. Tornabene, E. Viola, Generalized differential quadrature finite element method for vibration analysis of arbitrarily shaped membranes, International Journal of Mechanical Sciences, 79 (2014) 216-251.

[14] S. Moradi, H. Makvandi, D. Poorveis, K.H. Shirazi, Free vibration analysis of cracked postbuckled plate, Applied Mathematical Modelling, 66 (2019) 611-627.

[15] M. Ishaquddin, S. Gopalakrishnan, A novel weak form quadrature element for gradient elastic beam theories, Applied Mathematical Modelling, 77 (2020) 1-16.

[16] M.M. Navardi, Supersonic flutter analysis of thin cracked plate by Differential Quadrature Method, Master of Scince thesis, Amirkabir University of Technology University, Tehran, Iran (2015).

[17] Y. Wang, X. Wang, Y. Zhou, Static and free vibration analyses of rectangular plates by the new version of the differential quadrature element method, International Journal for Numerical Methods in Engineering, 59(9) (2004) 1207-1226.

[18] G. Karami, P. Malekzadeh, Application of a new differential quadrature methodology for free vibration analysis of plates, International Journal for Numerical Methods in Engineering, 56(6) (2003) 847-868.

[19] H. Shahverdi, M.M. Navardi, Free vibration analysis of cracked thin plates using generalized differential quadrature element method, Structural engineering and mechanics: An international journal, 62(3) (2017) 345-355.

[20] J.N. Reddy, Mechanics of laminated composite plates and shells: theory and analysis, CRC press, 2003.

[21] C.W. Bert, M. Malik, The differential quadrature method for irregular domains and application to plate vibration, International Journal of Mechanical Sciences, 38(6) (1996) 589-606.

[22] N. Bardell, The free vibration of skew plates using the hierarchical finite element method, Computers & structures, 45(5-6) (1992) 841-874.

[23] M. Zamani, A. Fallah, M. Aghdam, Free vibration analysis of moderately thick trapezoidal symmetrically laminated plates with various combinations of boundary conditions, European Journal of Mechanics-A/Solids, 36 (2012) 204-212.

[24] A.W. Leissa, The free vibration of rectangular plates, Journal of sound and vibration, 31(3) (1973) 257-293.

[25] R. Solecki, Vibration of a simply supported L-shaped plate, (1997).

[26] R. Solecki, Free-vibration of an L-shaped plate: the general solution and an example of a simply-supported plate with a clamped cutout, (1996).

[27] F.-L. Liu, K. Liew, Analysis of vibrating thick rectangular plates with mixed boundary constraints using differential quadrature element method, Journal of Sound and Vibration, 225(5) (1999) 915-934.

HOW TO CITE THIS ARTICLE

H. Shahverdi, M. M. Navardi, M. H. Sadr, A Proposed Approach to Simulate Thin Quadrilateral Plates Using Generalized Differential Quadrature Method Based on Kirchhoff–Love Theory, AUT J. Mech Eng., 6(1) (2022) 15-30.

DOI: 10.22060/ajme.2021.20283.5995